Military Technical College
Cairo, Egypt

12th International Conference on Applied Mechanics and Mechanical Engineering (AMME)
May 16-18, 2006

DYNAMIC BEHAVIOR OF CONTROL VALVES OF A LIQUID ROCKET ENGINE FEEDING SYSTEM

Tamer N. MAHMOUD*, M. Galal RABIE**, M. Allam EL-SENBAWI***

ABSTRACT

This paper presents a part of study conducted to investigate the dynamic behavior of a rocket propellant rocket engine. The part presented here concerns the modeling, simulation and analysis of the dynamic behavior of the hydraulic control valves of the feeding system of the studied rocket engine. The study involves the combustion chamber, the gas generator controller, the thrust regulator, and the relief valve. For the studied valves, non-linear mathematical models have been deduced and used to develop computer simulation programs. The study was extended to investigate the static and dynamic behaviors of the valves. The study showed that the combustion chamber and gas generator controllers act to produce a feeding fuel pressure equal to the oxidizer pressure. The thrust controller, through regulating the combustion chamber pressure, could keep a fairly constant thrust of the rocket engine. The developed simulation programs could be used for further investigation of the effect of the valves constructional and operational parameters as well as the study of dynamic behavior of the liquid propellant engine.

KEY WORDS

Control, valve, feeding system, rocket, engine, liquid, static, dynamic, behavior, computer, simulation.

---

* Captain Eng, Egyptian Armed Forces.
** Professor, Modern Academy for Engineering & Technology, Cairo, Egypt.
*** Maj. Gen. (R), Assoc. Professor, Egyptian Armed Forces.

NOMENCLATURE

A	Area, (m^2)
A_q	Combustion chamber controller poppet valve restriction area, (m^2)
A_o	Combustion chamber controller servopiston orifice area (m^2)
A_N	Thrust controller resultant poppet area, (m^2)
A_{ps}	Gas generator controller net piston area, (m^2)
A_{sf}, A_{sb}	Valve face and back areas of the safety valve, (m^2)
B	Bulk modulus of propellants, (Pa)
C_d	Discharge coefficient
C_c	Contraction coefficient
D_{m1}	Combustion chamber controller membrane clearance diameter, (m)
D_4	Valve diameter of the safety valve, (m)
d_v	Mean seat, poppet diameter of the thrust controller, (m)
E	Modulus of elasticity of membrane, (Pa)
f	Friction coefficient of moving parts, (N-s/m)
F_L	Limiter force, (N)
F_J	Combustion chamber controller momentum force, (N)
G	Modulus of material rigidity, (Pa)
h	Membrane thickness, (m)
K	Stiffness, (N/m)
K_s	Spring stiffness, (N/m)
K_{mb}	Membrane stiffness, (N/m)
K_{eqmb}	Equivalent stiffness of K_s and K_{mb}, (N/m)
m	Moving parts mass, (kg)
P	Pressure, (Pa)
Q	Volumetric flow rate, (m^3/s)
r	Membrane radius, (m)
V	Initial volume of chamber, (m^3)
X, y	Moving parts displacement, (m)
X_m, y_m	Moving parts maximum displacement, (m)
X_o, y_o	Spring pre-compression distance, preset membrane clearance, (m)
ρ	Density, (kg/m^3)
θ	Combustion chamber controller fuel flow angle, (rad)

SUBSCRIPTS

1	Combustion chamber controller membrane assembly
11	Combustion chamber controller servopiston assembly
2	Thrust controller
3	Gas generator controller
4	Safety valve
c	Combustion chamber
cc	Combustion chamber controller
cp	Clear piston
e	Exit
f	Fuel
g	Gas generator
gc	Gas generator controller
i	Inlet
iv	Inlet valve
L	Limiter of moving parts (LD= down, LL= left, LR = right, LU= upper)
mb	Membrane
o	Oxidizer
p	Pump
r	Rod
s	Safety valve
sp	Servopiston
tc	Thrust controller

1. INTRODUCTION

The simulation by digital computers plays an important role in the development and analysis of behavior of hydraulic control systems. It allows observing the variations of the operational parameters in the transient conditions. Moreover, it provides a powerful tool for the optimization of the constructional parameters of the studied systems. This paper deals with the static and dynamic behavior of hydraulic control valves of the feeding system of a liquid propellant rocket engine. The system involves a set of valves controlling the pressure and the flow rate of the fuel and oxidizer liquids. The valves have peculiar design imposed by the constraint that these two liquids should never come into contact outside the combustion chamber.

Actually, the available literature does not include any similar study. However, the library is rich with papers dealing with the classical and electrohydraulic control valves and systems. An exception was the work of Rabie[1], which dealt theoretically with the dynamic behavior of a pilot operated pressure reducer. This valve serves to produce a fuel pressure equal to the oxidizer pressure. Rabie also investigated the same valve performance[2] by developing a Black Bond graph model. However, the study of publications of Shin[3]; Manring[4], Margolis[5], and Furst[6] gave good support to the theoretical part of the present paper.

A schematic of the system investigated in the present work is shown in Fig.1. More detailed description of the system can be found in reference[7]. The system involves a combustion chamber controller, a gas generator controller, a thrust controller, and a safety valve. The study involves valve description, deduction of nonlinear mathematical model and the development of a computer simulation program for each element. The simulation is carried out using the SIMULINK simulation program. The effects of some operational and constructional parameters on the static and dynamic behaviors of the valves are investigated.

2. COMBUSTION CHAMBER CONTROLLER

2.1. Valve Description

Schematic of the combustion chamber controller is shown in Fig.2. The valve serves to control the fuel pressure, P_{fcce}, supplied to the combustion chamber fuel injectors, to be equal to the oxidizer control pressure, P_{op}. The fuel is supplied to the valve from a pump at high pressure, P_{fp}. The fuel flow in the valve is throttled by a poppet displaced by servopiston.

The valve is equipped with membrane that acts as a feedback element. It is subjected to the difference between the oxidizer pressure, P_{op}, and the exit fuel pressure, P_{fcce}. The membrane deforms to change the area of an orifice between the membrane center and its receiver, restricting the fuel flow Q_{fs} which reaches the servopiston chamber. The piston has an orifice, A_o, connecting the servopiston chamber with the drain chamber. If the exit fuel pressure decreases than the oxidizer pressure, the membrane moves in a direction tending to reduce the area of the membrane restrictor. The pressure in the servopiston chamber, P_{fs}, decreases and the servopiston moves to the right. This displacement increases the exit fuel flow rate and the fuel exit pressure to be equal to the oxidizer pressure, and the membrane regains its neutral position.

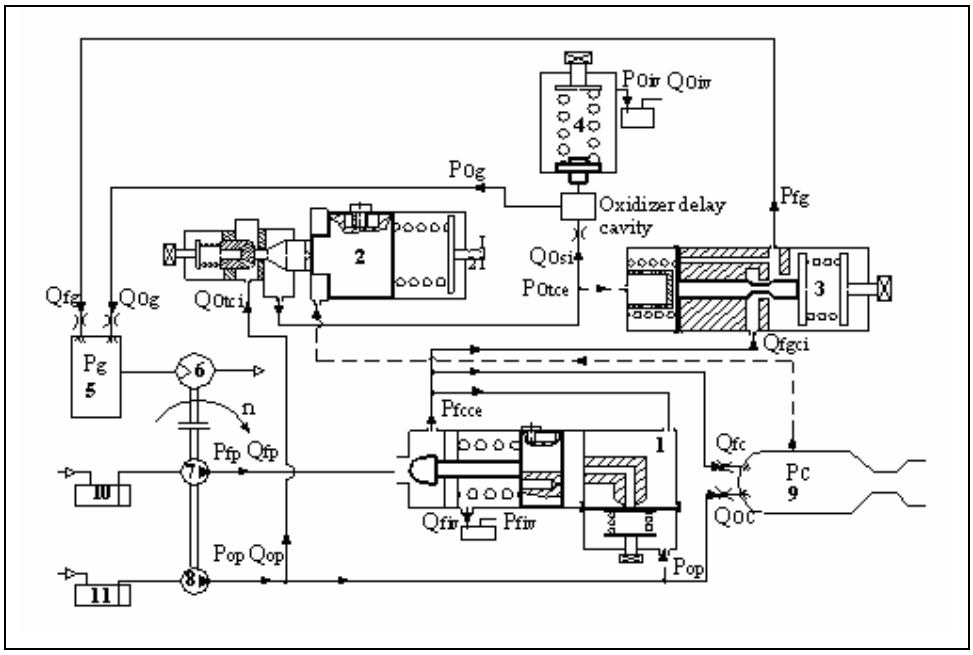

Fig.1 Schematic of the system assemblies

1. combustion chamber controller, 2. thrust controller 3. gas generator controller,
4. safety valve, 5. gas generator, 6. turbine, 7. fuel pump, 8. oxidizer pump,
9. combustion chamber, 10. fuel tank, 11. oxidizer tank.

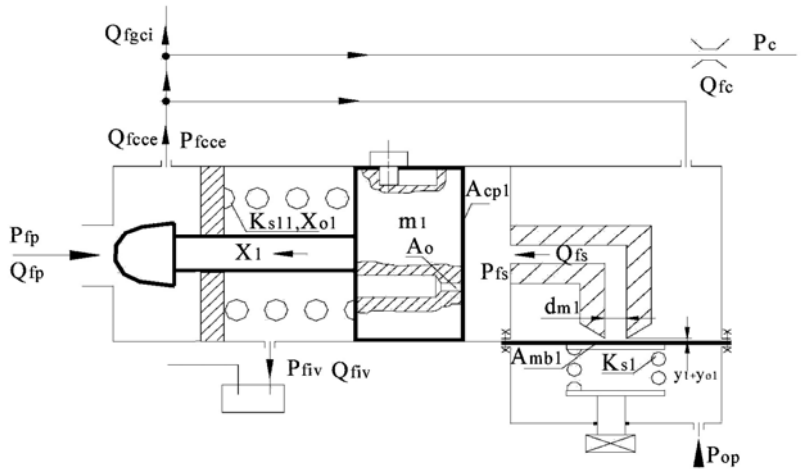

Fig.2. Scheme of combustion chamber controller
(pilot operated pressure reducer)

2.2. Mathematical Model

The static and dynamic behavior of the studied valve can be described by the following equations.

Flow rate through the main poppet valve

As seen from Fig.3, the restriction area of the main poppet valve, Aq(x1) changes nonlinearly with the poppet displacement (x1). Considering the dimensions of the

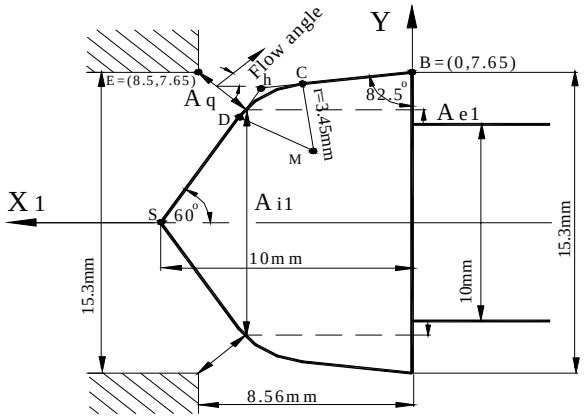

Fig.3 Profile of the controller poppet head

valve poppet and poppet seat, the valve throttle area (A_q), poppet area subjected to inlet pressure (A_{i1}), area subjected to exit pressure (A_{e1}) and flow angle were calculated. The calculation results are plotted in Fig.4. The flow through the poppet valve is given by:

$$Q_{fp} = C_d A_q(x_1)\sqrt{\frac{2}{\rho_f}(P_{fp} - P_{fcce})} \qquad (1)$$

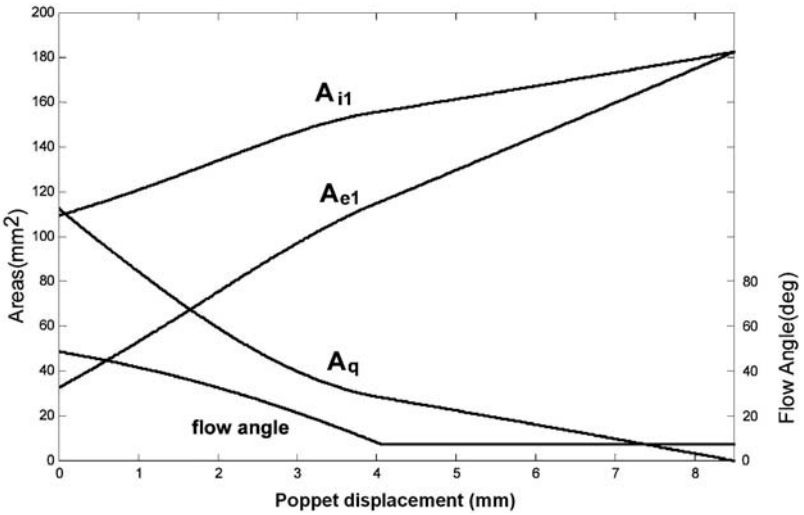

Fig.4. Variation of the profiled poppet head areas and flow angle

Flow rate through combustion chamber fuel injectors

The fuel flow rate to the combustion chamber equals to the summation of the flow rates through the individual injectors. The fuel flow rate is given by:

$$Q_{fc} = \sum_{i=1}^{n} C_{di} A_{fci} \sqrt{\frac{2}{\rho_f}(P_{fcce} - P_c)} \quad \text{or} \quad Q_{fc} = k\sqrt{(P_{fcce} - P_c)} \qquad (2)$$

Flow rate through orifice controlled by membrane displacement

The membrane clearance height, (y_1+y_{o1}), is too small compared with the receiver diameter d_{m1}. Therefore, the membrane controls a restriction gap of an area: $\pi d_{m1}(y_1+y_{o1})$. The flow through this restriction area is given by:

$$Q_{fs} = C_d \pi d_{m1}(y_{o1} + y_1)\sqrt{\frac{2}{\rho_f}(P_{fcce} - P_{fs})} \tag{3}$$

Flow rate through servo-piston orifice

$$Q_{fiv} = C_d A_o \sqrt{\frac{2}{\rho_f}(P_{fsp} - P_{fiv})} \tag{4}$$

Membrane displacement

The pilot oxidizer pressure influences the valve operation through the fixed edge metallic membrane. The membrane is loaded by forces due to the pilot pressure, the fuel exit pressure and the spring pre-compression. In the absence of the two pressures, the spring is pre-stressed to a pre-set membrane clearance (y_{o1}). When applying the loading pressure, $\Delta P=P_{fcce}-P_{op}$, the maximum deformation at the membrane center, (y_1), is given by the following expression [8]:

$$y_1 = \Delta P r_1^4 / (6E_1 h_1^3)$$

The equivalent membrane stiffness can be thus deduced as:

$$K_{mb1} = F_m / y_1 = \pi r^2 \Delta P / y_1 = 6\pi E_1 h_1^3 / r_1^2$$

The resultant membrane stiffness (K_{mb1}) and its adjusting spring (K_{s1}) is given by:

$$K_{eq_{mb1}} = K_{mb1} + K_{s1}$$

The equation of motion of the membrane is written as:

$$(P_{fcce} - P_{op})A_{mb1} = m_1 \frac{d^2 y_1}{dt^2} + f_1 \frac{dy_1}{dt} + K_{eq_{mb1}}(y_1 + y_{o1}) + F_{Lmb1} \tag{5}$$

Membrane displacement limiter force

$$F_{LUmb1} = \begin{cases} 0 & -y_1 < y_{m1} \\ (|y_1| - y_{m1})K_{L1} + f_{L1}\dfrac{dy_1}{dt} & -y_1 \geq y_{m1} \end{cases}$$

$$F_{LDmb1} = \begin{cases} (y_1 - y_{m1})K_{L1} + f_{L1}\dfrac{dy_1}{dt} & y_1 \geq y_{m1} \\ 0 & y_1 < y_{m1} \end{cases}$$

$$F_{Lmb1} = F_{LDmb1} - F_{LUmb1} \tag{6}$$

Continuity equation applied to exit chamber

The valve exit line is connected to the combustion chamber fuel injectors and feedback membrane chamber by means of a rigid tube of sufficiently large diameter. Consequently, they may be treated as a single chamber. The application of the continuity equation to the exit chamber yields:

$$Q_{fp} - Q_{fc} - Q_{fsp} - Q_{fgci} - \left(A_{i1}(x_1) - A_{r1}\right)\frac{dx_1}{dt} - \frac{dP_{fcce}}{dt}\frac{V_{e1} + A_{i1}(x_1)x_1 - A_{r1}x_1}{B} = 0 \qquad (7)$$

Continuity equation applied to servo-piston chamber

$$Q_{fsp} - Q_{fiv} - A_{cp1}\frac{dx_1}{dt} - \frac{dP_{fsp}}{dt}\left(\frac{V_{11} + A_{cp1}x_1}{B}\right) = 0 \qquad (8)$$

Equation of motion of servo-piston

$$P_{fsp}A_{cp1} - P_{fiv}\left(A_{cp1} - A_{r1}\right) + P_{fcce}A_{e1}(x_1) - P_{fp}A_{i1}(x_1) + F_{j1} = m_{11}\frac{d^2x_1}{dt^2} + f_{11}\frac{dx_1}{dt} + K_{s11}(x_1 + x_{o1}) + F_{L11} \qquad (9)$$

Servo-piston displacement limiter force

$$F_{LR11} = \begin{cases} \left(|x_1| - x_{m1}\right)K_{L11} + f_{L11}\dfrac{dx_1}{dt} & -x_1 \geq x_{m1} \\ 0 & -x_1 < x_{m1} \end{cases}$$

$$F_{LL11} = \begin{cases} x_1K_{L11} - f_{L11}\dfrac{dx_1}{dt} & x_1 \geq 0 \\ 0 & x_1 < 0 \end{cases}$$

$$F_{L11} = F_{LR11} - F_{LL11} \qquad (10)$$

Flow forces acting on the poppet valve

$$F_{j1} = \frac{\rho_f Q_{fp}^{\ 2}\cos\theta(x_1)}{C_C A_q(x_1)} \qquad (11)$$

2.3. Analysis of Dynamic Behavior

The combustion chamber controller is described mathematically by equations 1 to 11. A SIMULINK simulation program was developed on the basis of these equations and used to investigate the valve behavior.

Effect of membrane clearance

The pre-compression of the membrane spring is the only adjustable constructional parameters in this valve. The influence of this clearance on the precision of control of the exit pressure is studied by calculating the transient response of the valve for different values of (y_{o1}). The oxidizer pressure was kept constant (81 bar) in these calculations. The steady-state values of the exit fuel pressure are plotted against the

membrane clearance in Fig.5. This figure shows that the steady state value of fuel pressure is equal to that of oxidizer pressure. The initial membrane clearance has no significant effect on the precision of control of exit fuel pressure.

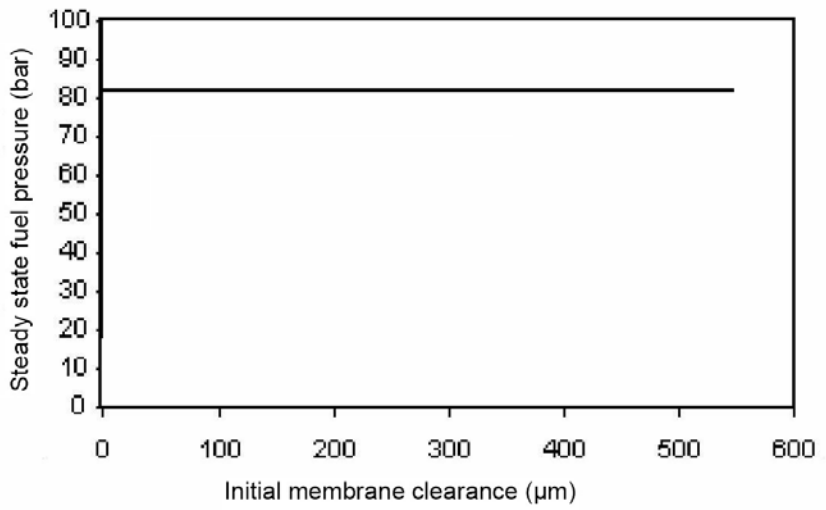

Fig.5. Variation of fuel exit pressure with membrane clearance variations

Controller response to step variations of pilot oxidizer pressure

The transient response of the valve exit pressure to step variations of the pilot oxidizer pressure is calculated by the simulation program and illustrated in Fig.6 and Fig.7. The figures show that the exit pressure reaches always a steady state value that equals to the pilot oxidizer pressure. The valve response is over damped. The greater the pilot oxidizer pressure step magnitude, the greater is the required piston travel to produce equal increase in the fuel exit pressure. Therefore the response time increases with the increase of the magnitude of the input step. The valve response to the pilot pressure reduction is faster than the case of its increase. The step response is of settling time less than 40ms. The response did not show, practically, any steady state error.

Controller response to step variations of input fuel pressure

The effect of variations of inlet fuel pressure on the precision of control of exit fuel pressure has been investigated. The transient response of the exit fuel pressure to step variations of the inlet fuel pressure of different magnitudes was calculated by the simulation program. The results are plotted in Fig.8. This figure shows that the exit fuel pressure reaches a steady state value equal to that of the control oxidizer pressure. The response did not show, practically, any steady state error. The results show also that the settling time of the valve is less than 3.5 ms.

The effect of variation of combustion chamber pressure on the precision of control of exit fuel pressure has been investigated. The transient response of the exit fuel pressure to step variations of the combustion chamber pressure of different magnitudes was calculated using the simulation program. The results are illustrated by Fig.9. This figure shows that the exit fuel pressure reaches a steady state value equal to that of the control oxidizer pressure. The response did not show, practically, any steady state error. The results show also the settling time of the valve is less than 10 ms.

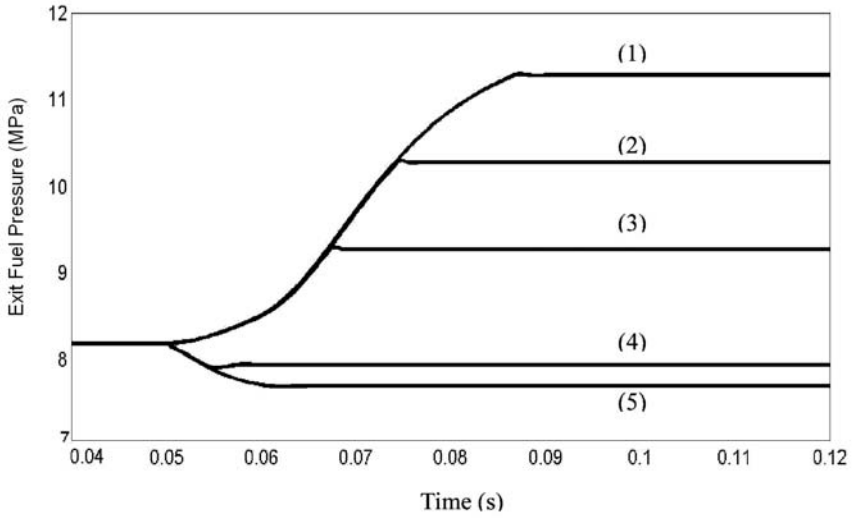

Fig.6. Response of the controller with fuel injectors to pilot oxidizer pressure step variations with (P_{fp} =8.85 MPa & P_c =5 MPa).
(1) P_{op} = 8.1 to 11.5 MPa, (2) P_{op} = 8.1 to 10.5 MPa,
(3) P_{op} = 8.1 to 9.5 MPa (4) P_{op} = 8.1 to 8.05 MPa,
(5) P_{op} = 8.1 to 7.9 MPa

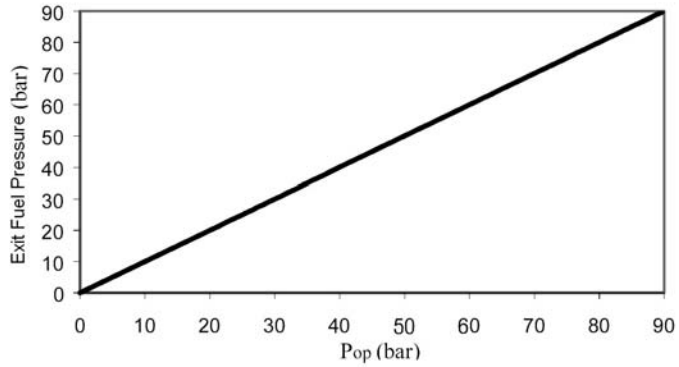

Fig.7. Relation between exit fuel pressure and oxidizer control signal

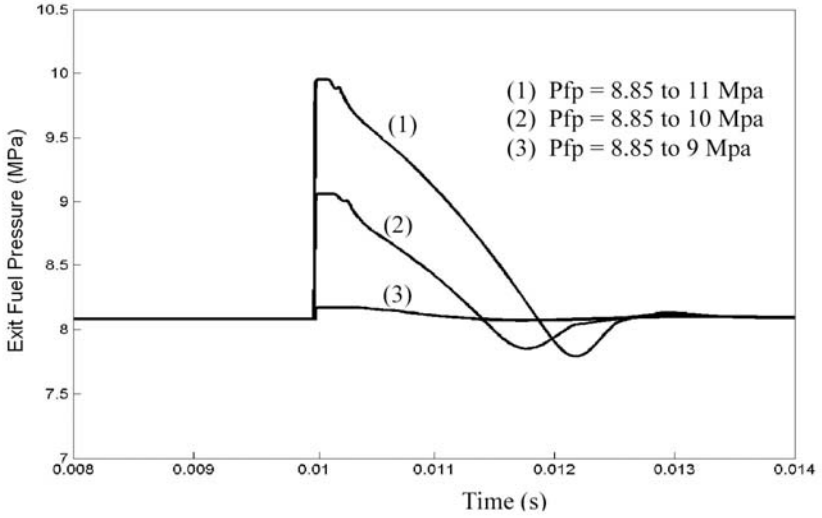

Fig.8. Response of the controller with fuel injectors to input fuel pressure step variations with (P_c = 5 MPa & P_{op} = 8.1 MPa).

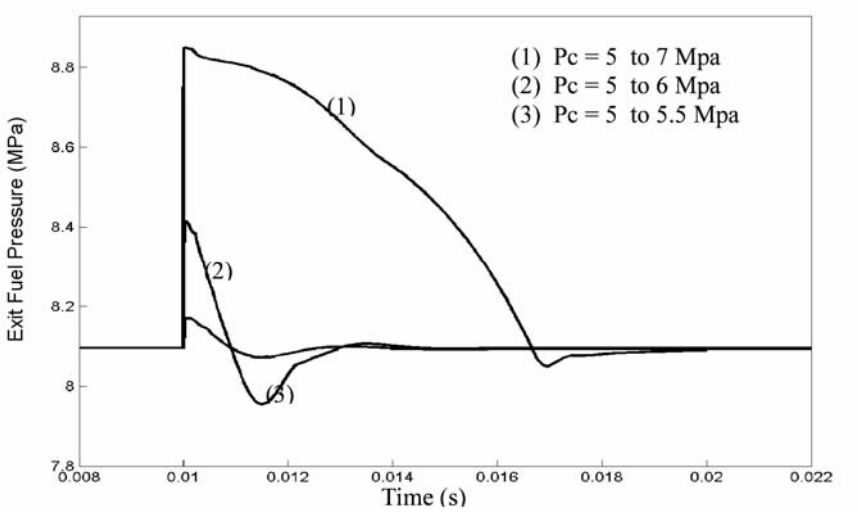

Fig.9. Response of the controller with fuel injectors to combustion chamber pressure step variations with (P_{op}=8.1 MPa& P_{fp}=8.85 MPa).

Effect of the poppet shape

The effect of the poppet shape on the valve response was investigated by calculating the valve step response for different poppet shapes. The studied valve has a poppet of too complicated shape. Actually, this shape was intended to produce certain behavior. Therefore, the decisions concerning any modification in the poppet shape should be supported by deep investigation of its effect on the valve response. When replacing the complicated shape of the poppet by a simple conical one, the step response of the valve changes. Figure 10 shows the step response of the valve considering its original geometry and for a simple conical poppet. The step increase in input oxidizer pressure from 9.5 to 10.05 MPs applied at (t=0.01s). The study of Fig.10 shows that when replacing the original shape by the simple conical one the settling time increases from 65 ms to 140 ms a steady state error 3% appears. Therefore, the original shape was selected to minimize the settling time and maximize the precision of control.

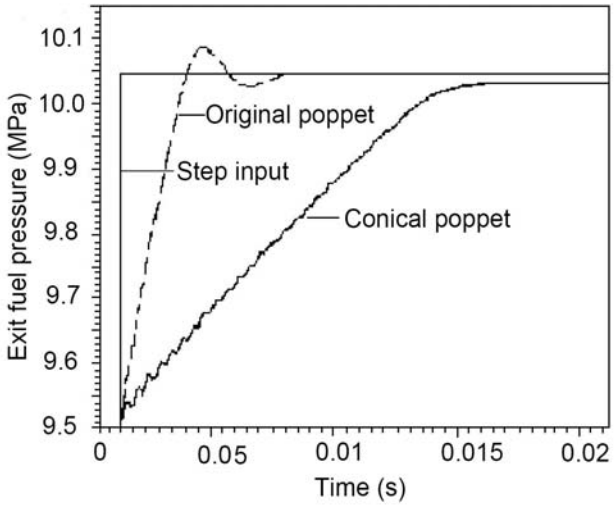

Fig.10. Effect of the poppet shape on the controller step response.

3. GAS GENERATOR CONTROLLER

3.1. Valve Description

Gas generator controller shown in Fig.11 serves to control the exit fuel pressure, P_{fg}, supplied to the gas generator fuel injectors. This pressure should be equal to the oxidizer control pressure, P_{otce}, that exits from the thrust controller. The fuel is supplied to the valve from the combustion chamber controller at pressure P_{fcce}. The fuel flow in the valve is throttled by a poppet valve. The throttling area A_{i3} is controlled by the displacement of diaphragm (3) displacement. The diaphragm is the feedback element. The poppet is constantly pressed to the diaphragm by a spring (7). The diaphragm is subjected to the difference between the oxidizer pressure, P_{otce}, and the exit fuel pressure, P_{fg}. When the exit fuel pressure increases more than the oxidizer pressure, the diaphragm deflects to move the poppet to reduce the throttling area. Consequently, the exit fuel pressure decreases to equal the oxidizer pressure.

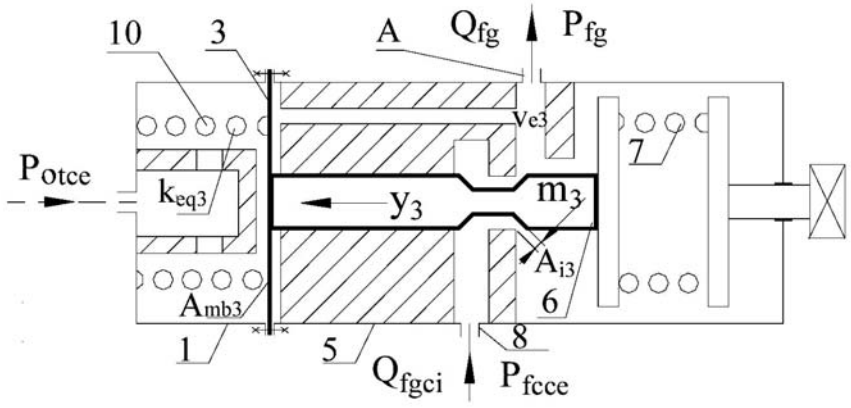

Fig.11. Scheme of gas generator controller (pilot operated pressure reducer)

3.2. Mathematical Model

The static and dynamic behavior of the studied valve can be described by the following equations.

Flow rate through throttling input area

The input fuel flow rate can be controlled by the variable throttling area, which changes non-linearly with the piston displacement. The fuel flow rate is given by:

$$Q_{fgci} = C_d A_{i3}(y_3)\sqrt{\frac{2}{\rho_f}\left(P_{fcce} - P_{fg}\right)} \tag{12}$$

Considering the geometry of the poppet valve, the following expression for the throttling area could be deduced.

$$A_{i3}(y_3) = 2.2214(0.0085 + 0.5y_3)(0.003 - y_3)$$

Flow rate through gas generator fuel injectors

The fuel flow rate supplied to the gas generator equals the summation of the flow rates through the individual injectors. The fuel flow rate is given by the following equations:

$$Q_{fg} = \sum_{i=1}^{n} C_{di} A_{fgi} \sqrt{\frac{2}{\rho_f}\left(P_{fg} - P_g\right)}$$

$$Q_{fg} = k_g \sqrt{\left(P_{fg} - P_g\right)} \tag{13}$$

Continuity equation applied to exit chamber

$$Q_{fgci} \_ Q_{fg} \_ \left(A_p\right)\frac{dy_3}{dt} - \frac{dp_{fg}}{dt}\frac{V_{e3}}{B} = 0 \tag{14}$$

Equation of motion of the moving parts

The pilot pressure (oxidizer pressure exit from thrust controller) influences the gas generator controller operation through the fixed edge metallic membrane. The membrane is loaded by the pilot oxidizer pressure, the exit fuel pressure and the spring. In the absence of the two pressures, the membrane is in its neutral position. When applying the loading pressure difference the maximum deformation at the membrane center is given by the following expression[8] .

$$y_3 = \Delta P r_3^{\,4} / \left(6 E_3 h_3^{\,3}\right)$$

The equivalent stiffness of the membrane is calculated by the following equation.

$$K_{mb3} = F_m / y_3 = \pi r_3^{\,2} \Delta P / y_3 = 6\pi E_3 h_3^{\,3} / r_3^{\,2}$$

The resultant stiffness of the membrane K_{mb3} and its adjusting spring K_{s3} are given by

$$K_{eq_{mb3}} = K_{mb3} + K_{s3}$$

Actually, the piston spring stiffness is negligible compared with the membrane stiffness.

$$\left(P_{fg} - P_{otce}\right) A_{mb_3} = m_3 \frac{d^2 y_3}{dt^2} + f_3 \frac{dy_3}{dt} + K_{eq_{mb3}} y_3 + F_{L_{mb3}} \tag{15}$$

Membrane displacement limiter force

The membrane displacement is limited mechanically, in both directions by the material of the thrust controller body. When the moving parts reach the maximum displacement, the displacement limiters act by counter forces to stop them. The displacement limiters are treated as stiff springs with considerable structural damping. The displacement limiters forces are given by the following expressions:

$$F_{LU3} = \begin{cases} (y_3 - y_{m3})K_{L3} + f_{L3}\dfrac{dy_3}{dt} & y_3 \geq y_{m3} \\ 0 & y_3 < y_{m3} \end{cases}$$

$$F_{LD3} = \begin{cases} (|y_3| - y_{m3})K_{L3} - f_{L3}\dfrac{dy_3}{dt} & -y_3 \geq y_{m3} \\ 0 & -y_3 < y_{m3} \end{cases}$$

$$F_{Lmb3} = F_{LD3} - F_{LU3} \qquad (16)$$

3.3. Analysis of Dynamic Behavior

Controller response to step variations of pilot oxidizer pressure

The response of the valve exit pressure to step variations of the pilot oxidizer pressure is calculated and illustrated in Figs.12 and 13. The figures show that the exit pressure reaches always steady state values equal to the oxidizer pressure. The greater the pilot oxidizer pressure the greater is the required piston travel required to produce equal increase in the exit fuel pressure. Therefore the response time increases with the increase of the magnitude of the input step. The valve response to the pilot pressure reduction is thus faster than the case of its increase. The step response is of settling time less than 2 ms, it did not show, actually, any steady state error.

Controller response to step variations of input fuel pressure

The effect of variations of inlet fuel pressure on the precision of control of exit fuel pressure has been investigated. The transient response of the exit fuel pressure to step variations of the inlet fuel pressure of different magnitudes has been calculated by the simulation program. The simulation results are plotted in Fig.14. This figure shows that the exit fuel pressure reaches a steady state value equal to that of the control oxidizer pressure. The transient responses have settling time less than 7 ms with no observable steady state error.

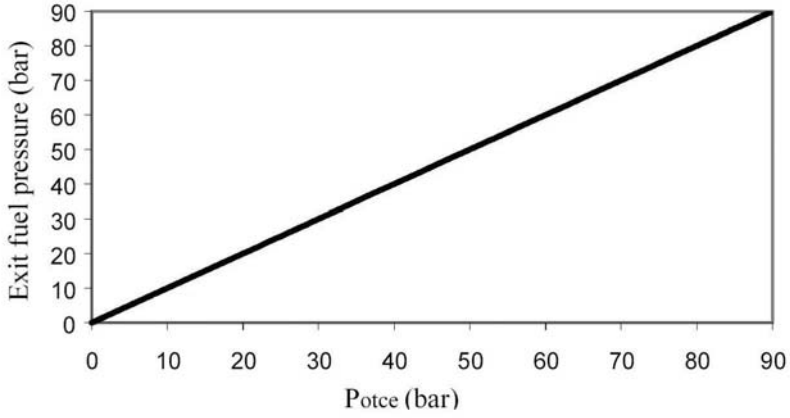

Fig.12. Steady state relation between exit fuel pressure and oxidizer pressure

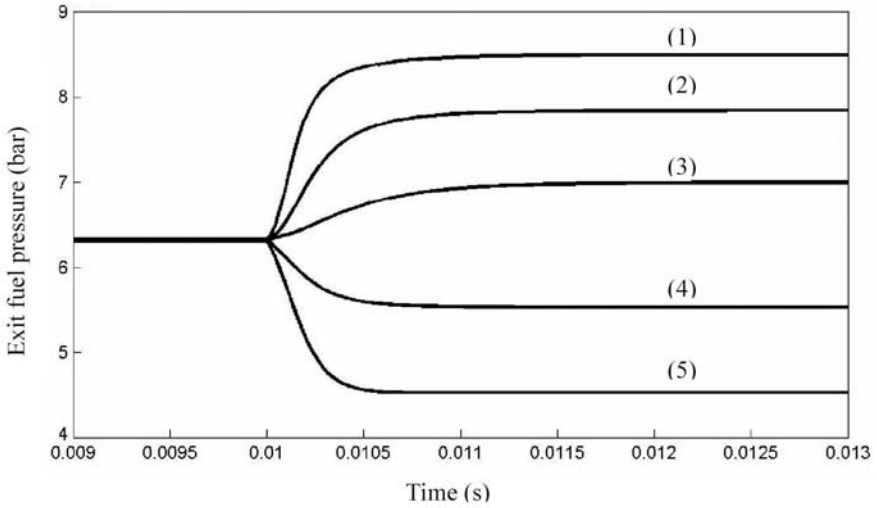

Fig.13 Response of the gas generator controller with fuel injectors to pilot oxidizer pressure step variations with (P_{fcce}=8.1 MPa & P_g=4.8 MPa)

(1) P_{otce} = 6.35 to 8.7 MPa (2) P_{otce} = 6.35 to 8 MPa
(3) P_{otce} = 6.35 to 7.1 MPa (4) P_{otce} = 6.35 to 5.75 MPa
(5) P_{otce} = 6.35 to 4.75 MPa

Controller response to step variations of gas generator pressure

The effect of variation of gas generator pressure on the precision of control of exit fuel pressure has investigated. The transient response of the exit fuel pressure to step variations of the gas generator pressure of different magnitudes has calculated. The results are illustrated by Fig.15. This figure shows that the exit fuel pressure reaches a steady state value equal to that of the control oxidizer pressure. The results show also the settling time of the valve is less than 3.5 ms.

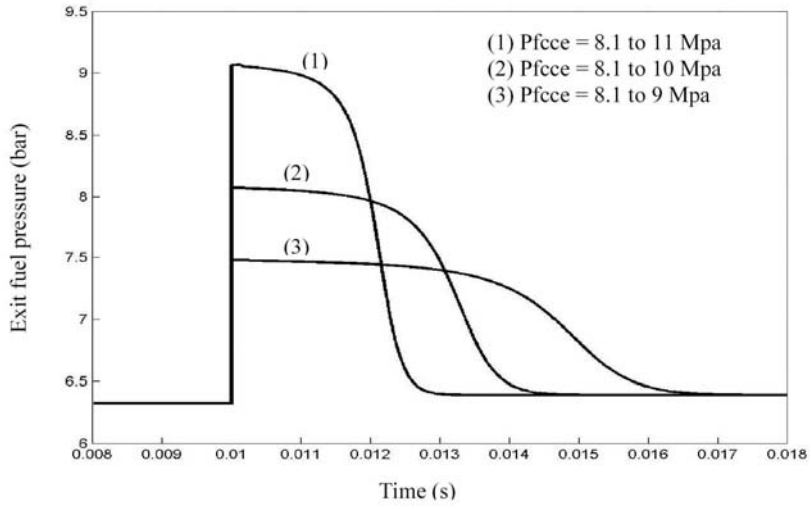

Fig.14. Response of the gas generator controller with fuel injectors to step variations of input fuel pressure with (P_{otce}=6.35 MPa & P_g=4.8 MPa).

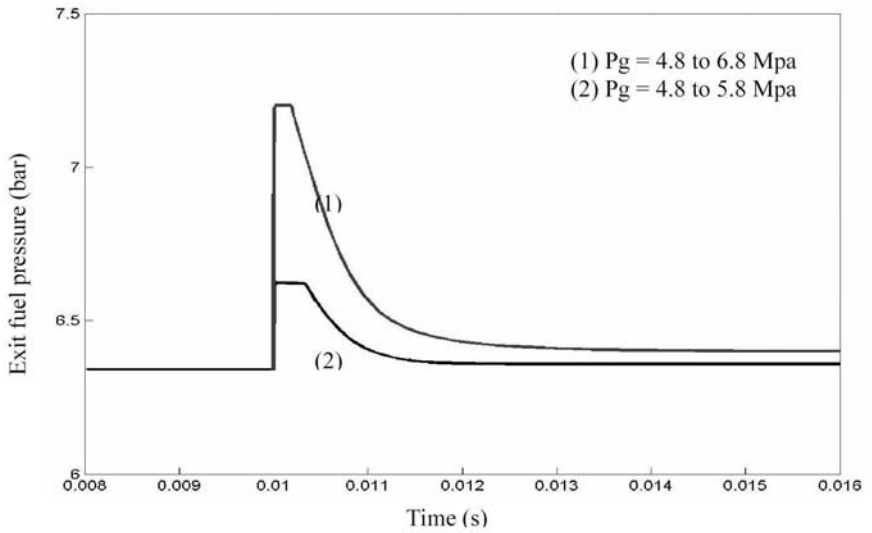

Fig.15. Response of the gas generator controller with fuel injectors to step variations of gas generator pressure with (P_{otce} = 6.35 MPa & P_{fcce} = 8.1 MPa).

4. THRUST CONTROLLER

4.1. Valve Description

Thrust controller, Fig.16, service to maintain the required pressure in the combustion chamber, P_c. It switches the rocket engine from first power rating to the second one. The oxidizer is supplied to the controller from a pump at high pressure, P_{op}. The oxidizer flow in the controller is throttled by a valve displaced by a poppet valve (4). The poppet rests against a piston (6) by means of auxiliary spring (1). The piston is a sensing element. It is subjected to the difference between the spring force and combustion chamber pressure force. The exit oxidizer flow is delivered to the gas generator injectors. When the combustion chamber pressure is increased, piston, poppet, and valve move against spring force causing the through section of the throttling slot, x_{m2}, to reduce. This results in a decrease of oxidizer flow rate to the gas generator and a drop of gas generator pressure. Turbine power and the speed of the pump drive assembly rotor go down. The pressure of liquid propellant components at the pump outlet and their consumption are decreased.

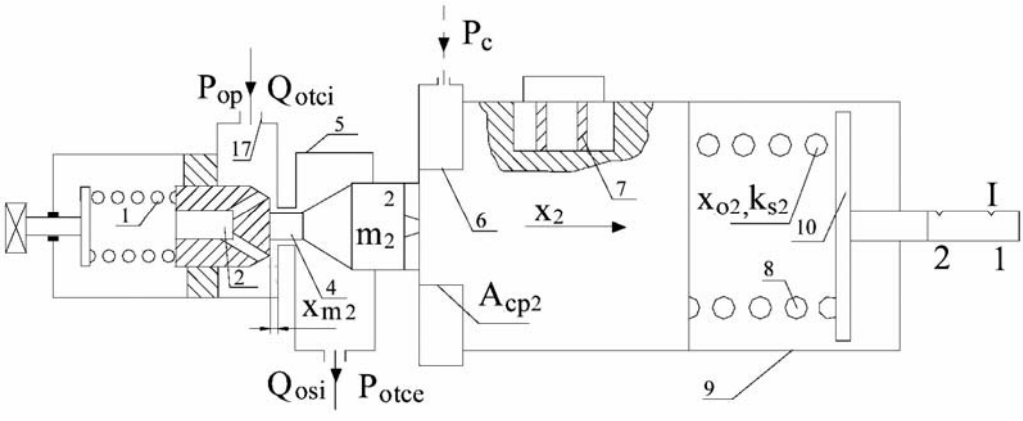

Fig.16. Scheme of thrust controller

The combustion chamber pressure drops to a preset value. When the engine is started the thrust controller is set for the first power rating. The setting is changed by two squibs with pyrocharge when the engine switches to the second power rating.

4.2. Mathematical Model

The static and dynamic behavior of the thrust controller valve can be described by the following equations.

Flow rate through valve orifice

The valve throttling space, (X_{m2}-X_2), is too small compared with the seat-poppet clearance. Therefore, the valve controls the restriction area, $\pi d_v(X_{m2}-X_2)$, and the displacement (X_2) is limited ($0<X_2<X_{m2}$). The controller inlet flow rate is given by the following equation.

$$Q_{otci} = C_d \pi d_v \left(X_{m2} - X_2\right)\sqrt{\frac{2}{\rho_o}\left(P_{op} - P_{otce}\right)} \tag{17}$$

Exit flow rate

The oxidizer that flows from the thrust controller is guided to the gas generator through safety valve of constant inlet throttling area. The following equation gives the flow rate through this orifice.

$$Q_{osi} = C_d A_{si}\sqrt{\frac{2}{\rho_o}\left(P_{otce} - P_{og}\right)} \qquad \text{Or} \qquad Q_{osi} = K_d\sqrt{P_{otce} - P_{og}} \tag{18}$$

Continuity equation applied to exit chamber

$$Q_{otci} - Q_{osi} - A_N\frac{dX_2}{dt} - \frac{V_{e2}}{B}\frac{dP_{otce}}{dt} = 0 \tag{19}$$

Equation of motion of the moving parts

$$P_c A_{cp2} + P_{otce} A_{e2} + P_{op} A_{i2} = m_2\frac{d^2X_2}{dt^2} + f_2\frac{dX_2}{dt} + K_{s2}\left(X_2 + X_{o2}\right) - F_{L2} \tag{20}$$

Moving parts displacement limiter force

The moving parts displacement is limited mechanically, from the left side by the thrust controller body and from the right side by the seat material. The seat reaction forces of the displacement limiters are given by the following equations.

$$F_{LL2} = \begin{cases} |X_2|K_{L2} - f_{L2}\dfrac{dX_2}{dt} & X_2 \le 0 \\ 0 & X_2 > 0 \end{cases}$$

$$F_{LR2} = \begin{cases} \left(X_2 - X_{m2}\right)K_{L2} + f_{L2}\dfrac{dX_2}{dt} & X_2 \ge X_{m2} \\ 0 & X_2 < X_{m2} \end{cases}$$

$$F_{L2} = F_{LL2} - F_{LR2} \tag{21}$$

4.3. Analysis of Dynamic Behavior

Effect of spring pre-compression length on the controller behavior

The pre-compression length of the thrust controller spring is the only adjustable constructional parameter in this valve. In the studied system, it is changed by means of special mechanism, powered by a pyro-charge. The transient response of the valve, for step variation of spring pre-compression of different values, has been calculated and plotted in Fig.17.

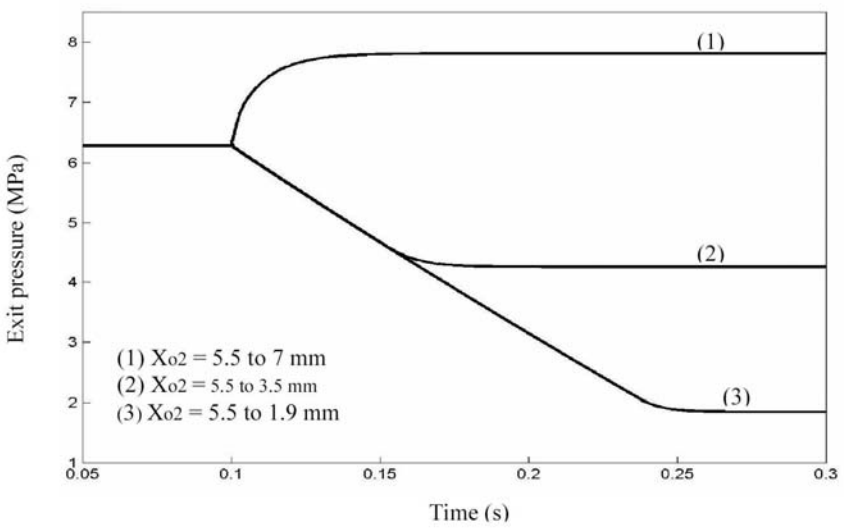

Fig.17. Response of the oxidizer pressure exit from the thrust controller to step variation of spring pre-compression length (P_{op} = 8.1 MPa & P_c = 5 MPa).

When the spring has a large pre-compression length the piston motion would be limited due to the opposite high spring force. The throttle area is large and the exit pressure is also high. Conversely, when the spring has a small pre-compression length, the area of the throttling space becomes smaller, which results in a decrease of the exit pressure values.

This explains why the thrust controller would act as a switcher from first power rating to the second one. When the engine is just starting, the controller operates at the first power rating. The setting of the controller is changed when the engine is changed over to the second power rating. The simulation results show that settling time of the valve is less than 150 ms.

Controller response to step variations of input oxidizer pressure

The response of the thrust controller exit pressure to step variations of the inlet oxidizer pressure is plotted in Fig.18. This figure shows when the inlet oxidizer pressure increases the exit oxidizer pressure increases, the combustion chamber pressure increases. The throttling area becomes smaller. The exit oxidizer pressure decreases and the combustion chamber restore its original maintained pressure. The results show the settling time of the valve is less than 30 ms.

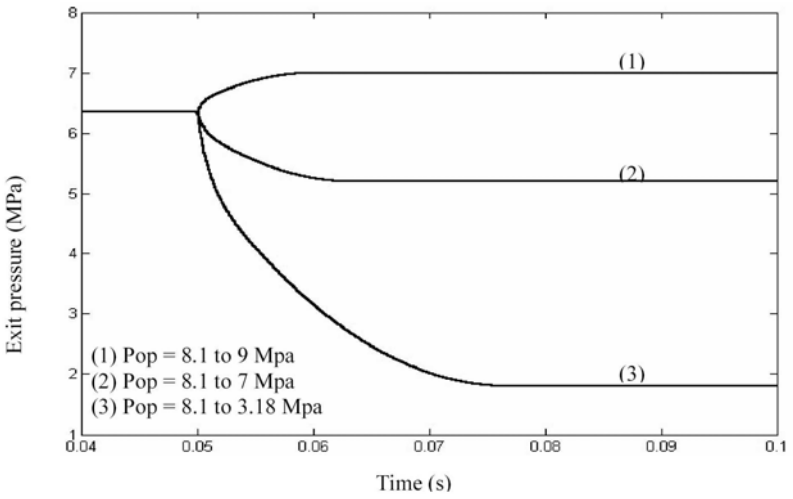

Fig.18. Response of the oxidizer pressure exit from the thrust controller to step variation of input oxidizer pressure (X_{o2}=5.5 mm & P_c=5 MPa)

.Controller response to step variations of combustion chamber pressure

The response of the thrust controller exit oxidizer pressure to the step variation of the combustion chamber pressure has been calculated. The results are illustrated in Fig.19. This valve operates to control and regulate the operating mode. If the combustion chamber pressure is increased, this valve operates to reduce the gas generator pressure, pump speed, fuel and oxidizer pressures in the direction to reach the predetermined combustion chamber pressure. The increase of combustion chamber pressure reduces the valve exit pressure by value proportional to the oxidizer pressure increment. The regulating and stabilizing effect of this valve is accomplished by closing the control loop in the whole feeding system circuit. The results show the settling time of the valve is less than 80 ms.

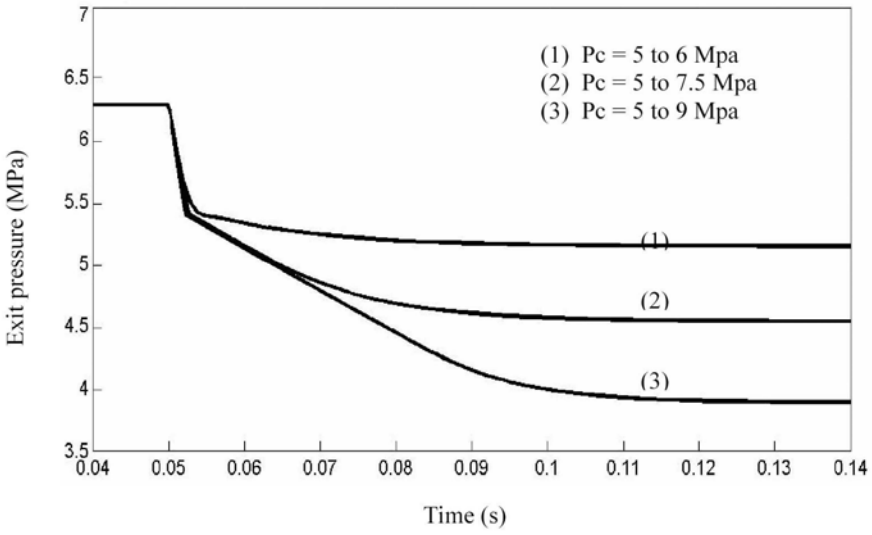

Fig.19. Response of the oxidizer pressure exit from the thrust controller to step variation of the combustion chamber pressure (Xo2=5.5mm & Pop=8.1 MPa).

5. SAFETY VALVE

5.1. Valve Description

The safety valve, Fig.20, acts to limit pressure of oxidizer fed to the injectors of the gas generator. It is equipped with an oxidizer delay cavity, which delays the delivery of oxidizer to the injectors of the gas generator during engine starting.

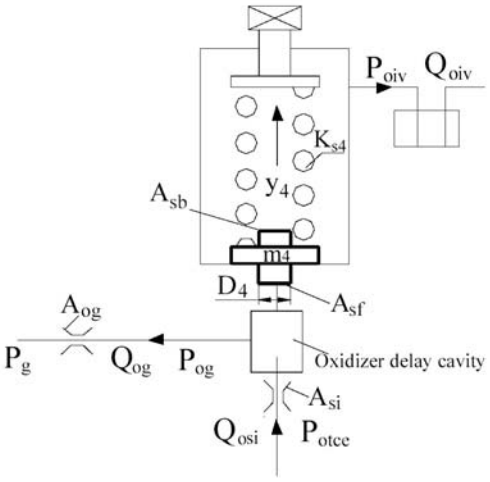

Fig.20. Scheme of safety valve

5.2. Mathematical Model

The static and dynamic behavior of the studied valve can be described by the following equations.

Flow rate through inlet orifice

The oxidizer flow rate inlet to the safety valve, Q_{oci}, is the flow rate exit from the thrust controller, described by equation (18).

Flow rate through gas generator oxidizer injectors

The oxidizer flow rate to the gas generator equals to the summation of flow rates through the individual injectors. The injectors' area can be replaced by an equivalent single orifice area. The oxidizer flow rate is described by the following equation:

$$Q_{og} = \sum_{i=1}^{n} C_{di} A_{ogi} \sqrt{\frac{2}{\rho_o}\left(P_{og} - P_g\right)} \quad \text{or} \quad Q_{og} = C_d A_{og} \sqrt{\frac{2}{\rho_o}(P_{og} - P_g)} \tag{22}$$

Flow rate through safety valve

If the oxidizer pressure increases to a certain value (67 bar), the safety valve starts to open to permit the oxidizer to flow into the oxidizer inlet valve. This action results in the reduction of the oxidizer pressure to the preset value. The oxidizer inlet valve flow rate can be calculated as follows.

$$Q_{oiv} = C_d \pi D_4 y_4 \sqrt{\frac{2}{\rho}\left(P_{og} - P_{oiv}\right)} \tag{23}$$

Continuity equation applied to valve chamber

$$Q_{osi} - Q_{og} - Q_{oiv} - A_{sf}\frac{dy_4}{dt} - \frac{V_{e_4} + A_{sf}y_4}{B}\frac{dP_{og}}{dt} = 0 \tag{24}$$

Equation of motion of moving parts

$$P_{og}A_{sf} - P_{oiv}A_{sb} + F_{L4} = m_4\frac{d^2y_4}{dt^2} + f_4\frac{dy_4}{dt} + K_{s4}(y_4 + y_{o4}) \tag{25}$$

Moving parts displacement limiter force

$$F_{L4} = \begin{cases} |y_4|K_{L4} + f_{L4}\dfrac{dy_4}{dt} & y_1 \le 0 \\ 0 & y_1 > 0 \end{cases} \tag{26}$$

The safety valve is described mathematically by equations 18, 22 to 26. These equations have been used as part of mathematical relation described the integrated feeding system of the rocket engine.

Valve response to step variations of input oxidizer pressure

The response of the safety valve exit oxidizer pressure P_{og} to variations of the input oxidizer pressure P_{otce} was calculated. The calculations were carried out keeping a constant value of exit throttling area A_{og}. The results are illustrated in, Fig. 21. The safety valve was adjusted to open at certain pressure value according to spring setting. The safety valve has a constant inlet throttling area. The response at high input oxidizer pressure values was highly oscillatory, and takes long time to reach a steady state value. The settling time of the valve in this case is less than 15 ms.

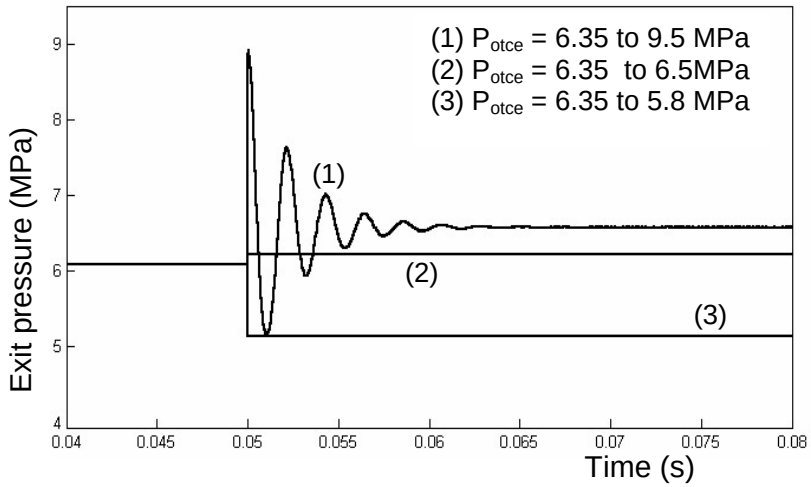

Fig. 21 Safety valve response to input oxidizer pressure step variations with (A_{og} = 5E-6 m^2)

Valve response to step variations of exit throttling area

The effect of the exit throttle area step variations A_{og} on the safety valve transient behavior with constant input oxidizer pressure P_{otce} is presented in Fig. 22. The figure shows that when the exit throttle area has a constant value, the exit oxidizer pressure has also constant value. When the exit throttling area steps down the exit oxidizer pressure increases. The settling time of the valve is less than 0.1 ms. When the exit throttle area step varied to zero the exit oxidizer pressure is equal to input oxidizer pressure value.

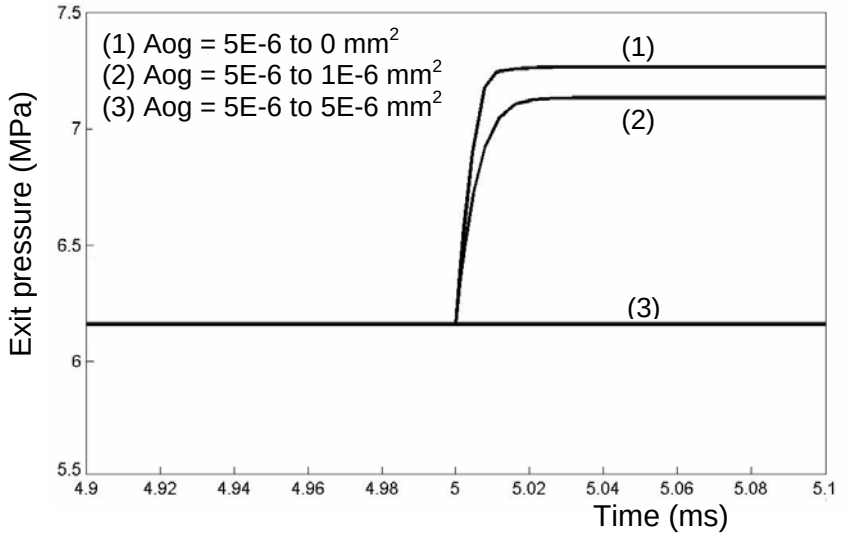

Fig. 22 Safety valve response to exit throttle area step variations with (P_{otce} = 6.35 MPa).

6. CONCLUSIONS

The simulation and analysis of behavior of hydraulic control valves of the feeding system of a liquid propellant rocket motor is carried out in this paper. Detailed mathematical models are developed. The models take into consideration the non-linear variation of areas as well as the non-linear pressure-flow relations describing the valves restrictions. The simulation is carried out using the SIMULINK simulation program. The following conclusions were reached from the study of simulation results:

(a) The non-linear behavior of the studied valves is clearly noticeable.

(b) The oxidizer pressure, controlled by the thrust controller, reaches stable steady state value corresponding to the manufacturer data. This valve shows an over damped response with settling time less than 150 ms.

(c) The fuel pressure controllers produce an output pressure equal to the pilot oxidizer pressure. The transient response of these valves is over damped. The settling time was found to be less than 40 ms.

(d) The developed simulation program could be applied for further analysis of the performance of the studied feeding system. Moreover, the production tolerances and allowances could be evaluated by using this program.

REFERENCES

1 Rabie, M. G., “Simulation and Analysis of a Pilot-Operated Hydraulic Pressure Reducer”, 3rd ASAT conference, Military Technical college, Cairo, 1-6 April, 1989, pp. 371-381

2 Rabie, M.G., and Hafez, H.E.; “Modeling by block bond graph and investigation of dynamic behaviour of a hydraulic pressure reducer” , Ain Shams University, Engineering Bulletin, vol. 26, no.1, Mars 1991, pp. 429-509.

3 Yung C.Shin; “Static and dynamic characteristics of a two stage pilot relief valve”, Journal of Dynamic Systems, Measurement and Control, vol. 113, no. 2, pp. 280-288, June 1991.

4 Manring, N.D., and Johnson, R.E.; “ Optimal orifice geometry for a hydraulic pressure-reducing valve”, Journal of Dynamic Systems, Measurements and Control, vol. 119, no. 3, pp.467-473, September 1997.

5 Margolis, D.L., and Hennings, C.; “Stability of hydraulic motion control system”, Journal of Dynamic Systems, Measurements and Control, vol. 119, no. 4, pp. 605-613, December 1997.

6 Furst, R.B., and Burgess, R.M.; “Small centrifugal pumps for low-thrust rockets”, J. propulsion, vol. 3, no. 3.

7 Tamer N. M. “Investigation of dynamic behavior of feeding system of liquid propellant rocket motor” M.Sc. Thesis, Military Technical College, Cairo, 2003.

8 Eshabach, O. W., “Handbook of Engineering Fundamentals”, J. W. NY, 1975.